Optical anisotropy in individual CdS quantum dot ensembles

Jifa Qi,* Chuanbin Mao, John M. White, and Angela M. Belcher
Department of Chemistry and Biochemistry, University of Texas, Austin, Texas 78712, USA
(Received 23 December 2002; revised manuscript received 30 April 2003; published 24 September 2003)

The polarized microphotoluminescence (PL) spectroscopy of individual spherical and rod-shaped CdS quantum dot (QD) ensembles has been investigated. In a spherical QD ensemble, optical anisotropy was observed despite the spherical shapes of both the ensemble and individual QD components. The directions of the maximum linearly polarized PL were different for different spherical QD ensembles, and independent on the polarization direction of the excitation. However, for a fixed polarization direction of PL, the PL yield significantly varied with the polarization direction of the excitation. In a rod-shaped QD ensemble, the direction of maximum polarized PL was observed to be perpendicular to the length direction of the rod, regardless of the polarization direction of the excitation. The observed PL anisotropies in individual spherical and rod-shaped QD ensembles are explained in terms of the crystallographic orientation of the individual QD components that make up the ensemble and obey the linear polarization selection rules. A statistic model is proposed to qualitatively describe the degree of polarization based on a three-dimensional crystallographic orientation of QDs with respect to the directions of excitation and observation.

DOI: 10.1103/PhysRevB.68.125319 PACS number(s): 78.67.Hc, 77.22.Ej, 78.55.Et

I. INTRODUCTION

Zero-dimensional semiconductor quantum dots (QD's), which can be considered as artificial atoms, have attracted considerable attention during the past decade for both the interests of fundamental physics and prospective applications.[1–3] It is well known that the inhomogeneities in sizes and shapes of the QD's are the causes of the optical spectral broadening of QD ensembles, since the energy of eigenstate in a QD strongly depends on the QD's size and shape. In fact, all the physical properties of a QD ensemble are measured as the average of the characteristic properties over all individual QD's. As a result, information about the individual components of the ensemble is obscured. Just as the shapes and sizes of the individual components are important factors in dealing with the physical properties of the QD ensemble, the crystallographic orientation of the individual QD's, in particular, preferential orientation of individual QD's is important for the study of optical anisotropy. The optical anisotropies of a QD ensemble with oriented individual QD's are different from those with randomly oriented individual QD's. For example, a spontaneous polarization has been theoretically predicted in an ideally oriented QD crystal.[4,5]

While photoluminescence (PL) provides information about electronic energy levels, the polarization of the emitted light reveals additional information about the electronic states. In bulk semiconductors, the study of polarization of PL has been an efficient tool for obtaining information about the symmetry of emission states and on the relaxation process of excited carriers. The optical anisotropy of individual QDs can be due to either their non-cubic crystalline structure or to their nonspherical shape, since the polarization depends on the symmetry of the wave function. Many polarized PL studies have been performed for individual quantum dots[6–9] and ensembles of dots.[10–12] Because the optical transition dipole of a QD has three-dimensional orientation with respect to the excitation light and observation, a three-dimensional probe of polarized emission from a single QD has been reported recently.[8,9] Similarly, the polarized emission from a QD ensemble is also a three-dimensional problem, that the crystallographic axis of each individual is three-dimensionally oriented with respect to the excitation and observation directions. In fact, the reported degree of polarization (DP) of a QD ensemble is usually smaller than that of a single QD. This is because that in a QD system with a large number of QD's, the DP is measured as an average result of all individual QD directions for both the excitation and the emission process. In addition, the anisotropic shape of the ensemble of closely packed QD's may also contribute to the optical anisotropy.[13] Therefore, it is worthwhile to investigate the optical anisotropy in specifically shaped QD ensembles in order to understand the involved physical processes.

In this paper, we present experimental PL observations for individual QD ensembles comprised of $\sim$2.5 nm diameter spherical quantum dots of CdS. The ensembles are themselves either spherical (100 to 300 nm diameter) or rod shaped. For a given spherical ensemble the PL is anisotropic and the anisotropy is independent of the polarization of the optical excitation. Rod-shaped ensembles exhibit a maximum PL intensity in the direction perpendicular to the long axis of the ensemble, independent of the incident polarization. The results are consistent with preferential crystallographic orientation of individual QD's within a given ensemble.

II. EXPERIMENTAL

A. CdS QD ensembles and TEM characterizations

The spherical and rod-shaped CdS QD ensemble samples used in the present work were prepared by a novel cold treatment process that provided control over the shapes of the closely packed QD ensembles independent of the kinds of II-VI materials. The spherical CdS QD ensembles were formed by the solidification of CdS QD solution at

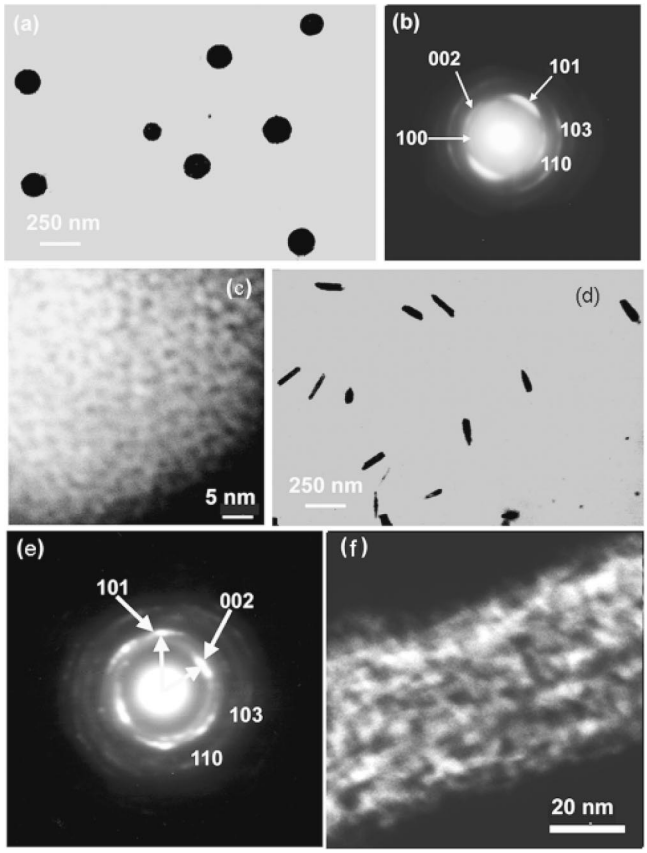

FIG. 1. (a) TEM bright field image of spherical QD ensembles. (b) ED pattern of an individual spherical QD ensemble showing the preferential orientation. (c) High magnification, high angle annular dark field (HAADF) STEM image of the spherical QD ensemble showing the nanocrystalline structure of the sphere. (d) TEM bright field of rod-shaped QD ensembles. (e) ED pattern of an individual rod-shaped QD ensemble, suggesting a preferential orientation with *c* axis parallel to the rod length direction, two reciprocal vectors for (002) and (101) from one single crystal are shown with arrows. (f) High magnification HAADF STEM image of the rod-shaped QD ensemble.

$-25\,^{\circ}\mathrm{C}$, while the rod-shaped QD ensembles were formed by aging the CdS solution at $0\,^{\circ}\mathrm{C}$. Details about the sample preparation were reported in Ref. 14. The transmission electron microscopy (TEM) characterizations were performed on a field emission electron microscope (JEOL product JEM-2010F) operating at 200 kV. The TEM samples were prepared by dispersing spherical or rod-shaped CdS QD ensembles on a carbon film supported grid.

Figure 1 shows the TEM images, electron diffraction (ED) patterns and scanning TEM (STEM) images of spherical and rod-shaped QD ensembles. The bright field TEM image of the spherical QD ensembles [Fig. 1(a)] shows the diameter of the individual spherical QD ensembles ranging from 110 to 300 nm, and the average size being 170 nm. Figure 1(c) shows a STEM image of a part of an individual spherical QD ensemble. STEM observation indicates that the QD ensembles were formed by almost spherical nanocrystals with the aspect ratios of $\sim 1.0-1.1$ and an average diameter of 2.5 nm. The interdot center distances were $\sim 3-4$ nm. ED patterns taken from an individual ensemble [Fig. 1(b)] clearly show that the QD's inside a spherical ensemble were wurtzite structured and their crystallographic axes were preferentially oriented. Figure 1(d) shows a low magnification TEM image of several rod-shaped QD ensembles with the length ranging from 150 to 200 nm and a mean width of 50 nm. ED patterns taken from an individual rod [Fig. 1(e)] show that the rod consisted of the wurtzite structured CdS QD's that were preferentially oriented with their [001] axis parallel to the rod length direction. The arrows in the ED pattern denote the reciprocal vectors corresponding to the crystallographic planes (101), (002) of one QD with [001] parallel to the rod. Figure 1(f) shows a STEM image taken from an individual rod, indicating that the rod was made up of closely packed QD's.

B. PL measurements

PL measurements were performed on the QD ensembles transferred onto a silicon (100) wafer. The silicon wafer with QD ensembles was mounted in a continuous-flow liquid-He cryostat. The linearly polarized second harmonic wave of a mode locked Ti:sapphire laser with 5-ps pulse width was used as the excitation source. A half-wave plate was used to rotate the polarization direction of the laser beam. A conventional far-field micro-PL system was used to collect the PL signal. The emitted light was collected through a micro-objective and a polarization analyzer. The PL light was detected by an Acton 0.5 m monochromator equipped with a liquid-nitrogen-cooled charge-coupled-device (CCD) array detector mounted on the exit port of the imaging spectrograph. A depolarizer was placed in front of the entrance slit of the monochromator in order to cancel out the polarization dependent response of the monochromator and the detector. All measurements were repeatedly taken on the same QD ensembles and all PL spectra were corrected for the spectral response of the apparatus. The resolution of the PL emission spectra is 0.1 meV. The sample was excited with 3.5 eV light with an intensity of about 200 $\mathrm{mW/cm^2}$ at 5 to 7 K.

III. RESULTS AND DISCUSSION

A. Optical anisotropic properties in individual spherical QD ensembles

Typical optical absorption spectra of spherical QD ensembles at room temperature are shown in Fig. 2. The optical absorption band edge of spherical QD ensembles shifted to a higher energy compared with that of bulk CdS material ($E_g = 2.43$ eV at room temperature). The blueshift of the absorption spectrum suggests the optical absorption spectroscopy of QD ensembles is dominated by the nanometer-sized constituent particles. This agrees with previous observations on other QD ensemble systems.[15] The PL spectrum of a single spherical QD ensemble consisted of a broad emission band with a width of 0.6 eV at half maximum (Fig. 2). The asymmetric shape of the PL spectra and the broad emission band suggested that the PL emission processes of the QD ensemble were complicated. The PL emissions at the higher energy side, corresponding to the PL spectral peak, originate prima-

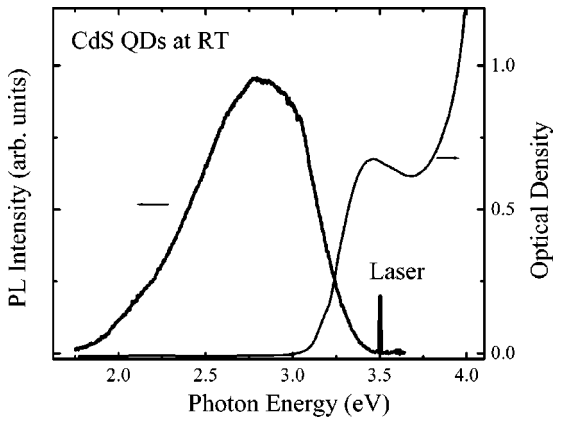

FIG. 2. Typical optical absorption spectrum (thin line) of a CdS spherical QD ensemble sample and the PL spectrum (thick line) of a spherical CdS QD ensemble at room temperature.

rily from the transitions of confined excited carriers. The PL emissions at the lower energy region, corresponding to the PL spectral tail, arise from the radiative transition at surface trap sites. Consequently, the broad PL emission band results from effects of the inhomogeneous size distribution of QD's,[16,17] the radiative transitions of surface trap states, and the interdot coupling of the closely packed QD's. A large Stokes shift of the emission band from the absorption edge was observed in the sample (Fig. 2). In addition to the general reason that the electron-phonon coupling effect caused the Stokes shift, the interaction between the QD's may also contribute to this additional red shift. The emission peak energy of the coupled QD's was reported to be lower than that of the well-isolated QD's.[15,17,18]

Since the QD's are wurtzite structured and preferentially oriented in the spherical QD ensemble, optical anisotropy is expected in the sample. Figure 3(a) shows the linearly polarized PL spectra of a single spherical QD ensemble detected

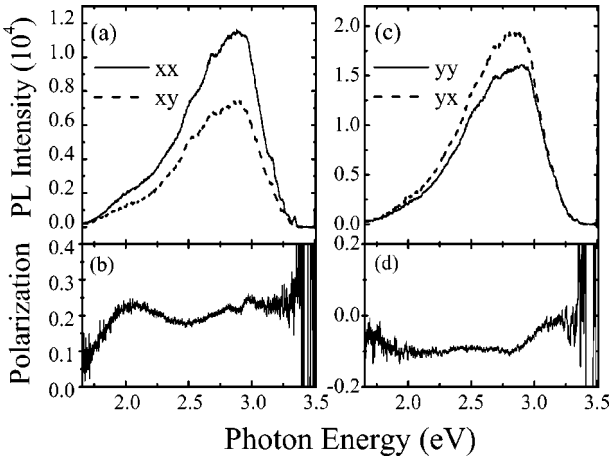

FIG. 3. (a) Micro-PL spectra of a spherical CdS QD ensemble in (*XX*) and (*XY*) polarization directions, respectively. (b) Degree of polarization of the PL spectra shown in the (a). (c) Micro-PL spectra of a spherical QD ensemble at (*YX*) and (*YY*) polarization directions, respectively. (d) Degree of polarization of the PL spectra shown in (c).

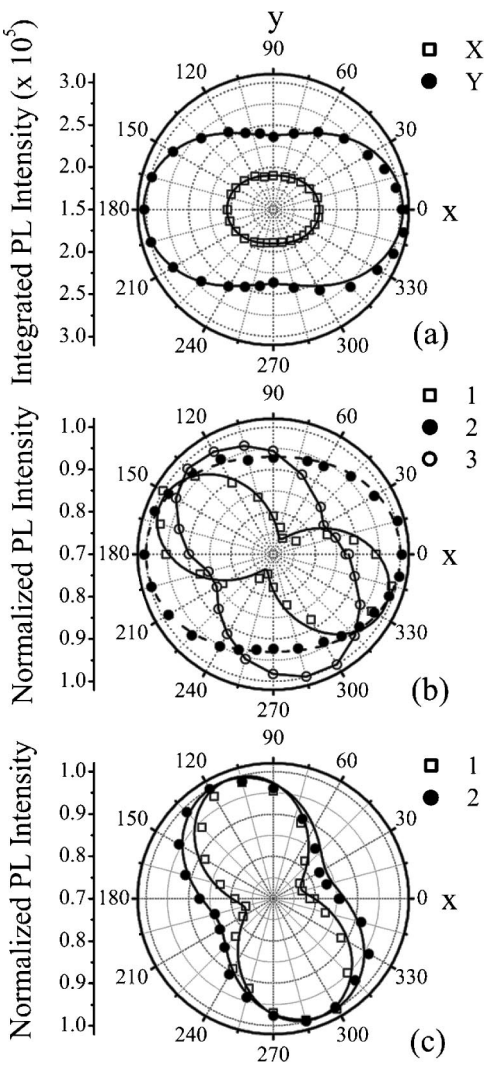

FIG. 4. (a) Polar plots of the integrated polarized-PL intensities in a spectral range from 2.516 to 3.046 eV from a spherical QD ensemble under a linearly polarized excitation in the *X* direction (squares) and *Y* direction (circles). (b) Polar plots of the integrated polarized-PL intensities from different spherical QD ensembles under the linearly polarized excitation in the *X* direction. The PL intensities were integrated in a spectral range from 2.516 to 3.046 eV and normalized to their maximum polarized intensities. The lines are to guide the eye. (c) Polar plots of the polarized-PL intensities at 2.866 eV (squares) and 2.128 eV (circles) from a spherical QD ensemble under the linearly polarized excitation in the *Y* direction.

for polarization parallel (*XX*) and perpendicular (*XY*) to that of the excitation light. Figure 3(c) shows the linearly polarized PL spectra of the components (*YX*) and (*YY*). In the denotations, the first and second coordinate represent the linear polarization direction of the excitation light and the PL light, respectively. The *z*-axis direction is parallel to the progression direction of the laser and the luminescence collection when using the confocal measuring mode. It is clearly seen that the PL yields at a given energy position varied with the polarization directions of the excitation and emission [Figs. 3(a) and 3(c)]. Figures 3(b) and 3(d) show the DP of the emission from the QD ensemble as a function of the

emission energy. These results show that the PL of the spherical QD ensemble was optically anisotropic. The origin of the polarization does not come from the geometric shapes of the individual QD's and the ensemble, but the preferential orientation of the wurtzite structured QD's. It is known that there are three valence bands $\Gamma_9(A)$, $\Gamma_7(B)$, and $\Gamma_7(C)$ in wurtzite structured CdS of C_{6v} symmetry. The electric dipole transition between the $\Gamma_9(A)$ and Γ_7 conduction band is allowed only for $\boldsymbol{E}\perp$ c polarized light. The electric dipole transition between the $\Gamma_7(B,C)$ valence bands and Γ_7 conduction band is allowed for both $\boldsymbol{E}\perp c$ and $\boldsymbol{E}\|c$. Here, c is the crystallographic axis and $\boldsymbol{E}$ is the electric field of light. The selection rule determines the polarization behavior of bulk CdS, also that of individual spherical CdS QD's. The optical anisotropy in a spherical CdS QD arises from the anisotropy of transition dipole moments for $\boldsymbol{E}\perp c$ and $\boldsymbol{E}\|c$ polarized light. Thus, the observed optical anisotropy in a spherical QD ensemble is considered as the average effect of all individual QD's.

To understand how the optical anisotropy in an individual QD affects the optical anisotropy in a QD ensemble, the polarized PL spectroscopy of individual spherical QD ensembles was investigated in detail. Figure 4(a) shows the polar plots of integrated PL intensities detected at different polarization directions from an individual spherical QD ensemble. The PL intensities were integrated in a spectral range from 2.516 to 3.046 eV, where the dominant emissions were due to the confined carriers. Two closed curves describe the polarized PL intensity as the function of polarization direction when excited by polarized light in X (circles) and Y (squares) direction. Obviously, the maximum of polarized PL intensities were in the same direction regardless of the excitation polarization direction. The polarized PL intensities at a fixed polarization direction varied with the polarization direction of the excitation. In addition, the directions of the maximum PL intensities were different for different spherical QD ensembles [Fig. 4(b)], which is considered to be due to the different preferential orientation direction of each individual ensemble with respect to observation.

Note all the data shown in Fig. 4(b) was collected from the spherical QD ensembles on the same substrate, which were synthesized by the same procedures. This leads one to believe that the QD's in those individual ensembles have the same orientation distribution. The difference of the DP values shown in Fig. 4(b) can be considered resultant of the fact that the experimental geometry is different for each individual spherical QD ensemble.

Here, we introduce a simple statistic model to describe the three-dimensional optical anisotropic in QD ensembles. Since the absorption probability of a wurtzite structured QD depends on the crystallographic orientation of the QD to the polarization direction of the excitation, QD's of different orientations in an ensemble are not equally excited. The emission from a QD excited by linearly polarized light is partially polarized. In a QD ensemble, the DP is determined by the orientation relaxations of the excited carriers and the average over all individual QD directions for both the excitation and the emission process. Assume the dipole oscillators of QD's are preferentially oriented in z-axis direction, the excitation electric field is located in the xz plane with an angle γ with the z axis, and the observation is carried out in the xy plane in direction of the angle β with the y axis. The orientation of an arbitrary oscillator is determined by the polar angle θ and the azimuthal angle φ. The excitation electric field has the form of $\boldsymbol{E}=(E\sin\gamma,0,E\cos\gamma)$. The induced dipole moment components are

$$p_x\sim(\boldsymbol{p}\cdot\boldsymbol{E})\sin\theta\cos\varphi, \tag{1}$$

$$p_y\sim(\boldsymbol{p}\cdot\boldsymbol{E})\sin\theta\sin\varphi, \tag{2}$$

$$p_z\sim(\boldsymbol{p}\cdot\boldsymbol{E})\cos\theta. \tag{3}$$

Correspondingly, the components of the luminescence intensity with the electric vector perpendicular to the xy plane and parallel to this plane are

$$I_\parallel\sim\langle p_z^2\rangle; I_\perp\sim\langle p_x^2\cos^2\beta+p_y^2\sin^2\beta\rangle. \tag{4}$$

Here, $\langle F\rangle$ is the average value of function F, defined by

$$\langle F\rangle=\frac{\int_0^{2\pi}\int_0^{\pi/2}Ff(\theta)\sin\theta d\theta d\varphi}{\int_0^{2\pi}\int_0^{\pi/2}f(\theta)\sin\theta d\theta d\varphi}, \tag{5}$$

where $f(\theta)$ is the probability that a QD emitter oriented at the angle θ. The DP that is defined by $P=(I_\parallel-I_\perp)/(I_\parallel+I_\perp)$ is the function of θ,γ and β, and is given by

$$P(\theta,\gamma,\beta)=\frac{\langle 8\cos^4\theta\cos^2\gamma-2\sin^4\theta\sin^2\gamma\sin^2\beta-\sin^4\theta\sin^2\gamma-4\sin^2\theta\cos^2\theta\cos 2\gamma\rangle}{\langle 8\cos^4\theta\cos^2\gamma+2\sin^4\theta\sin^2\gamma\sin^2\beta+4\sin^2\theta\cos^2\theta+\sin^4\theta\sin^2\gamma\rangle}. \tag{6}$$

Therefore, the DP value of a QD ensemble depends on the crystallographic orientations of QD's with respect to the polarization direction of the excitation and observation direction. The observation results of anisotropic PL emission behavior can be understood in terms of the preferential orientations of the QD's which agree with the TEM observations.

As mentioned above, the asymmetric broad PL spectra with a long PL tail extending well below the bulk band gap, shown in Fig. 2 and Figs. 3(a) and 3(c), are caused by the

contributions of inhomogeneous sizes of QD's and surface traps. It is necessary to see the contributions of the carriers that are confined in QD's and trapped by the surface defects. Figure 4(c) shows the polar plots of the polarized PL intensities at two representative energies of 2.866 and 2.128 eV, where the dominant recombination processes were caused by the confined carriers and surface traps, respectively. Obviously, the maximum polarized PL intensities at different photon energies were in the same direction, but the degrees of polarization were different. The calculated DP values of the emission at 2.866 and 2.128 eV from Fig. 4(c) were 0.13 and 0.10, respectively. The difference in the values of DP suggests that different origins of the emissions have different optical anisotropy. The polarization orientation of the emission from carriers at surface traps is understood by the polarization memory of the carriers, which relaxed to the surface trap states from the core states. Due to the polarization relaxation process, the degree of polarization of the emission from the trap states is lower than that of core states.

Another physical process may have also made the problem of optical anisotropy in a QD ensemble complex, since the effect of electronic interactions between the QD's exists in a QD ensemble with closely packed QD's.[15,17–20] Here, we will discuss two different situations: the crystallographic directions of the QD components in an ensemble are either randomly oriented or preferentially oriented. If the ensemble consisted of randomly oriented and closely packed QD's, the optical anisotropy may be observed in the ensemble. The optical anisotropy should show following behavior because of the symmetry and shape of the ensemble. (1) For a spherical QD ensemble, the direction of maximum of polarized PL should depend on the polarization direction of excitation. (2) For a rod-shaped QD ensemble, the maximum polarized PL may be in the direction that parallel to the long axis direction of rod, or depend on the direction of excitation, but never be normal to long axis direction of rod and independent of the excitation. Obviously, the first situation of the spherical QD ensemble is contrary to above observation results. In next section, we will show that the second situation of a rod-shaped QD ensemble is also contrary to the experimental observation. The facts support that the optical anisotropy in the spherical QD assembles is resultant of the crystallographic orientation of QD's. In the case that QD components are oriented, the anisotropic electric dipole of coupled quantum dots can be considered as the sum of the contributions of all the individual QD components. The individual QD's should have different contributions to the electronic dipole of coupled dots in the ensemble due to their orientation directions with respect to that of the excitation and the collection.

B. Optical anisotropy in individual rod-shaped QD ensembles

Above, we have described the optical anisotropy in individual spherical QD ensembles, and attributed it to the crystallographic orientations of individual QD's in the spherical ensemble. Since the anisotropic shape of the ensemble with closely packed QD's may also be the origin of optical anisotropy,[13] it is worthwhile to study the optical anisotropy in a rod-shaped QD ensemble in order to understand the origin of the optical anisotropy in QD ensembles.

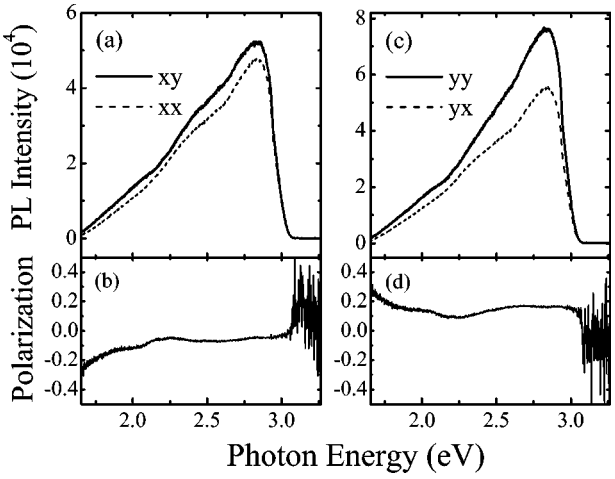

FIG. 5. (a) Micro-PL spectra of rod-shaped QD ensemble in (*XX*) and (*XY*) polarization directions respectively. (b) Degree of polarization of the PL spectra shown in the (a). (c) Micro-PL spectra of QD solid rod at (*YX*) and (*YY*) polarization directions, respectively. (d) Degree of polarization of the PL spectra shown in (c).

Figures 5(a) and 5(c) show the polarized micro-PL spectra of a rod-shaped QD ensemble in (*XX*), (*XY*), (*YX*), and (*YY*) polarization directions respectively. Figures 5(b) and 5(d) demonstrate the DP as the function of photon energy calculated based on the PL spectra shown in Figs. 5(a) and 5(c). Obviously, the polarized PL yields varied with the polarization directions of the emission and the excitation. Therefore, the individual rod-shaped QD ensemble exhibits the anisotropic PL. Figure 6 shows the polar plots of the integrated polarized-PL intensities from an individual rod-shaped ensemble under a linearly polarized excitation in the *x*-axis direction (squares) and in the *y*-axis direction (circles), re-

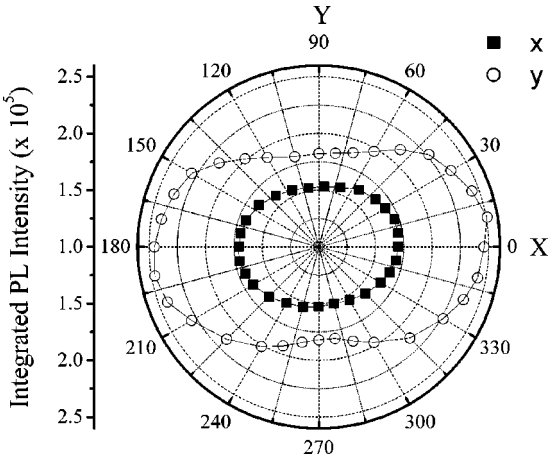

FIG. 6. Polar plots of the integrated polarized-PL intensities from the same single rod-shaped QD ensemble of Fig. 5 under a linearly polarized excitation in the *X* direction (squares), or perpendicular to the rod-shaped QD ensemble, and in the *Y* direction (circles), or parallel to the rod-shaped QD ensemble, respectively. The lines are to guide the eye.

spectively. The direction of maximum polarized PL is observed to be perpendicular to the length direction of the rod. It means that the polarized PL has its maximum in the direction that is perpendicular to *c* axes of QD's, since the crystallographic *c* axis was found to be parallel to the length direction of the rod in TEM observation. In addition, the anisotropy PL observation also reveals that the direction of maximum PL intensity changed for different rods since the rods are directed randomly on the Si substrate.

Due to the anisotropic shape and the quantum confinement effects, the optical anisotropy in nanorods or quantum wires has attracted much research.[13,21–24] A well-accepted theory of the optical anisotropy observed in nanowires/rods is based on the anisotropic dielectric constants between the nanorod and surrounding media.[13,23,24] According to this theory, when the electric field of light is parallel to the wire, no modulation takes place on the local electric field; when the electric field of light is normal to the rod axis, the local field is attenuated. As a result, the polarized PL along the long axis direction is stronger than that in the direction normal to the long axis of the rod.

Obviously, the optical anisotropy observed in our nanorods is different from the previously reported results of the optical anisotropy in nanowires or rods.[13,23,24] Our results showed that the polarized PL is stronger in the direction normal to the long axis of the rod. This fact suggests that the origin of optical anisotropy of our rod-shaped QD ensemble is different from the previous results where the optical anisotropy arises from the dielectric constant difference between the nanowire and its surrounding media, but the same as that of the spherical QD ensemble. That is, it arises from the crystallographic orientation of the QD's in the systems.

In conclusion, optical anisotropy is observed in both the individual spherical and rod-shaped QD ensembles. The QD's in the ensembles possess noncubic wurtzite crystalline structures, and consequently the anisotropy of transition dipole moments. The PL anisotropy in individual QD ensemble systems (sphere or rod) is the result of the average over all individual QD directions that are preferentially oriented with respect to both the excitation and the emission process.

ACKNOWLEDGMENTS

The authors would like to acknowledge the Beckman Foundation, the Welch Foundation and the University of Texas start-up funds for financial support. Texas Materials Institute Core Microscopy Facilities were used for TEM analysis. We also thank Professor K. Shih and the Keck Foundation for PL instrument time.

*Electronic address: jifa@mit.edu

[1] A.D. Yoffe, Adv. Phys. **42**, 173 (1993).
[2] L.E. Brus, Appl. Phys. A: Mater. Sci. Process. **53**, 465 (1991).
[3] A.P. Alivisatos, A.L. Harris, N.J. Levinos, M.L. Steigerwald, and L.E. Blus, J. Chem. Phys. **89**, 4001 (1988).
[4] K. Kempa, D.A. Broido, and P. Bakshi, Phys. Rev. B **43**, 9343 (1991).
[5] P. Lavallard and R.A. Suris, Solid State Commun. **95**, 267 (1995).
[6] M. Sugisaki, H.W. Ren, S.V. Nair, K. Nishi, S. Sugou, T. Okuno, and Y. Masumoto, Phys. Rev. B **59**, 5300 (1999).
[7] V. Zwiller, L. Jarlskog, M.E. Pistol, C. Pryor, P. Castrillo, W. Seifert, and L. Samuelson, Phys. Rev. B **63**, 233301 (2001).
[8] S.A. Empedocles, R. Neuhauser, and M.G. Bawendi, Nature (London) **399**, 126 (1999).
[9] I. Chung, K.T. Shimizu, and Moungi G. Bawendi, Proc. Natl. Acad. Sci. U.S.A. **100**, 405 (2003).
[10] P. Yu, W. Langbein, K. Leosson, J.M. Hvam, N.N. Ledentsov, D. Bimberg, V.M. Ustinov, A.Y. Egorov, A.E. Zhukov, A.F. Tsatsul'nikov, and Yu.G. Musikhin, Phys. Rev. B **60**, 16 680 (1999).
[11] A.L. Efros, Phys. Rev. B **46**, 7448 (1992).
[12] M. Chamrro, C. Gourdon, and P. Lavallard, J. Lumin. **70**, 222 (1996).
[13] C. B. Mao, C. E. Flynn, A. Hayhurst, R. Sweeney, J. Qi, J. Williams, G. Georgiou, B. Iverson, and A. M. Belcher, Proc. Natl. Acad. Sci. U.S.A. **100**, 6946 (2003).
[14] C. B. Mao, J. Qi, and A. M. Belcher, Adv. Funct. Mater. **13**, 648 (2003).
[15] C.B. Murray, C.R. Kagan, and M.G. Bawendi, Science **270**, 1335 (1995).
[16] S. Empedocles and M.G. Bawendi, Acc. Chem. Res. **32**, 389 (1999).
[17] C.R. Kagan, C.B. Murray, and M.G. Bawendi, Phys. Rev. B **54**, 8633 (1996).
[18] F. Gindele, R. Westphäling, U. Woggon, L. Spanhel, and V. Ptatschek, Appl. Phys. Lett. **71**, 2181 (1997).
[19] G.S. Solomon, J.A. Trezza, A.F. Marshall, and J.S. Harris, Jr., Phys. Rev. Lett. **76**, 952 (1996).
[20] S. Nagaraja, J.P. Leburton, and R.M. Martin, Phys. Rev. B **60**, 8759 (1999).
[21] J. Wang, M.S. Gudiksen, X. Duan, Y. Cui, and C.M. Lieber, Science **293**, 1455 (2001).
[22] J. Hu, L. Li, W. Yang, L. Manna, L. Wang, and A.P. Alivisatos, Science **292**, 2060 (2001).
[23] E.A. Muljarov, E.A. Zhukov, V.S. Dneprovskii, and Y. Masumoto, Phys. Rev. B **62**, 7420 (2000).
[24] J. Qi, A. Belcher, and J.M. White, Appl. Phys. Lett. **82**, 2616 (2003).